International Compressor Engineering Conference School of Mechanical Engineering

1976

Fatigue and Fracture Mechanics Properties of Valve Steels

R. Dusil

B. Appell

FATIGUE AND FRACTURE MECHANICS PROPERTIES OF VALVE STEELS

Robert Dusil and Bo Appell
Steel Research Center, Uddeholms Aktiebolag, Sweden

1 SUMMARY

S-N curves are presented for reversed bending and fluctuating tensile fatiguing of UHB 20C and UHB Stainless 716 cold rolled valve steel, strip thickness 0.30 mm (0.012 in) ultimate tensile strength approx. 1 900 MN/m^2 (280 ksi). Under fluctuating tensile loading, comparable fatigue limits are obtained for both steels after 2 x 10^6 loading cycles. Reversed bending gave higher fatigue limit for the stainless steel with 0.35 % C, 13 % Cr and 1 % Mo as compared to the 1 % C steel. The difference seems to stem from dissimilarities in composition, structure and in the nature of the surface, which has a great effect on the results of bending stress application.

UHB 20C with standard surface finish exhibited the same fatigue properties under reversed bending as tumbled material. It appears that the surface quality of the valve steel in the delivered condition is decisive in determining the suitability of the material for a given application, irrespective of edge quality.

Results from bending fatigue tests carried out on valve steels UHB 15M containing 0.74C and UHB 20C thickness 1.25 mm (0.049 in) and 1.0 mm (0.039 in), respectively, are presented.

Some basic concepts associated with fatigue and the testing methods which were used are described briefly. The importance of specimen preparation prior to the fatigue testing of high-strength material is dealt with.

The study is supplemented with crack growth data for valve steel and a determination of the material's fracture toughness at a strip thickness of 0.30 mm.

R. Dusil is Manager, Mechanical Properties, Steel Research Center, Uddeholms Aktiebolag, S-683 01 Hagfors, Sweden.
B. Appell is Manager, Product Development, Strip Division, Uddeholms Aktiebolag, S-684 00 Munkfors Sweden.

Some viewpoints on the problem of cold rolled steel strip fatigue are presented and the relevance of the obtained data for the application of the valve material is commented upon.

2 INTRODUCTION

The performance of a valve reed in a compressor is affected by a large number of factors, such as the design of the reed, loading geometry, material, ambient atmosphere etc. A study of failed valves showed that most of the valves failed due to fatigue (1, 2). The problem of fatigue concerns both the designer and the material manufacturer, whose goal is to manufacture material possessing optimal external and internal properties for the application in question. The external properties of a product such as steel strip are flatness, straightness, surface finish, dimensional tolerances etc. Internal properties have to do with analysis, structure and inclusion content, mechanical properties etc.

It is in the interest of the material manufacturer to analyse and quantify the above-mentioned properties in order to be able to meet the designer's material requirements. The present work presents a brief review of the fatigue and fracture mechanics properties of the valve steel.

3 GENERAL ON FATIGUE

3.1 Fundamental concepts

The term fatigue refers to the crack initiation and propagation which results when a material is subjected to repeated load. The maximum applied load is lower than the ultimate tensile strength of the material. The fatigue load can be fluctuating or reversed (see Fig. 1). Fluctuating bending is most common in flapper valve applications. The diagram in Fig. 2 defines some of the fatigue terms.

The results indicate that there is a limit stress which the material in question can withstand through an infinite number of loading cycles.

This limit is called the fatigue limit. In practical testing, the fatigue limit is defined for a given number of loading cycles, which in this case was 2 x 10^6. The property is statistically distributed and several different methods are used for its evaluation. In this work, the so-called staircase method (3, 4) is used. This method assumes that the fatigue limit is normal distributed property.

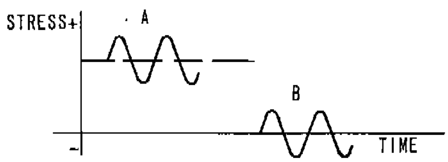

Fig. 1 Fluctuating (A) and reversed (B) stress.

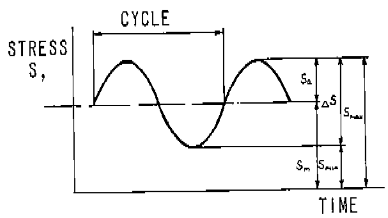

MEAN STRESS $S_m = \frac{S_{max}+S_{min}}{2}$

STRESS AMPLITUDE $S_a = \frac{S_{max}-S_{min}}{2}$

STRESS RATIO $R_s = \frac{S_{min}}{S_{max}}$

RANGE OF STRESS $\Delta S = S_{max}-S_{min}$

Fig. 2 Definition of fatigue terms.

If testing is carried out at a higher stress amplitude than that which corresponds to the fatigue limit and if the stress is plotted as a function of the number of loading cycles to fracture, a so-called S-N curve (Wöhler diagram) is obtained, Fig. 3. If S_a is plotted as a function of S_m, a Goodman (Smith) diagram is obtained (Fig. 4).

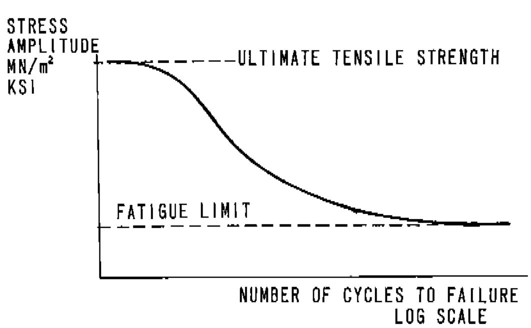

Fig. 3 S-N curve (Wöhler diagram).

3.2 Fatigue - phenomenological

Interest will now be concentrated on high-strength strip material with an ultimate tensile strength higher than 1 800 MN/m^2 (260 ksi). The fatigue limit of high-strength material is lower than its yield point, which means that cyclic deformation hardening does not take place throughout the whole specimen. However, a cyclic deformation hardening does take place in limited volumes of the material due to stress concentration around notches. These mechanisms are of fundamental importance for crack initiation and crack growth.

- Crack initiation

A local stress elevation which occurs around a notch (stress-raiser) can give rise to a plastic zone. The initiation of a fatigue crack in this zone is assumed to be controlled by the size of the plastic deformation. The crack can be considered to be initiated when the stress intensity factor range attains a threshold value, ΔK_T, see Fig. 5.

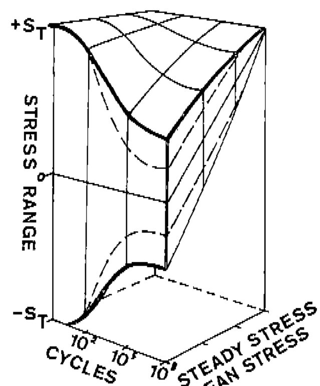

Fig. 4 Goodman (Smith) diagram.

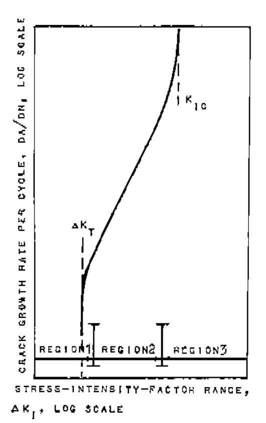

Fig. 5 Schematic representation of fatigue crack growth.

- Stable crack growth

When the crack has been initiated, i.e. when it has attained such a length that its growth is controlled by the variation of the stress intensity factor, stable crack growth occurs. The crack growth rate da/dN can, according to Paris (5), be described as

$$da/dN = C(\Delta K)^n \qquad \text{equ. 1}$$

a Crack length
N Number of cycles
ΔK Stress intensity range
C,n Empirical constants

- Unstable crack growth

If the crack grows to such a size that the fracture toughness K_c of the material is reached, the material fails spontaneously.

4 MATERIALS

Uddeholm hardened and tempered strip steels, specially manufactured to meet the requirements for compressor valve application, were used in this study. The nominal chemical composition is given in Table 1 below.

Table 1

GRADE	C	Si	Mn	Cr	(wt%) Mo
UHB 15M	0.74	0.24	0.75	-	-
UHB 20C	1.00	0.20	0.40	0.15	-
UHB Stainless 716	0.35	0.40	0.45	13.5	1.0

The temperature dependence of the ultimate tensile strength of the UHB 20C and UHB Stainless 716 is shown in Fig. 6. The materials were tested in as delivered condition and tempered at 200°C (400°F) 100 and 1 000 hours respectively.

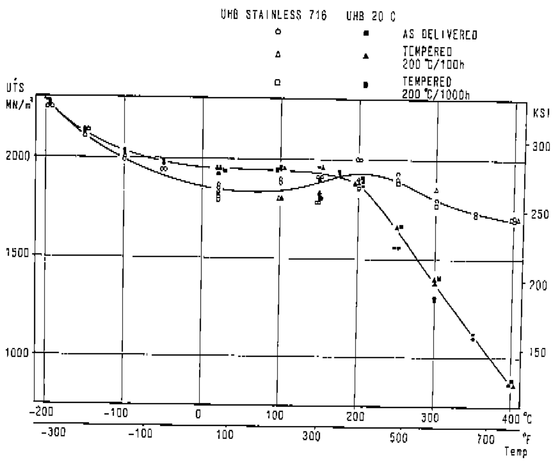

Fig. 6 Tensile strength versus temperature, UHB 20C and UHB Stainless 716, thickness 0.30 (0.012 in).

Additional information concerning Uddeholm cold rolled valve steels can be found in ref. (7).

5 FATIGUE TESTING - EXPERIMENTAL

5.1 Fluctuating and reversed bending

Machine: SONNTAG SF-2-U, testing frequency 30 Hz, maximum vibration force 0 to 125 ± 125 N. The machine is equipped with a mechanical oscillator which drives the vibration arm, whose movement is transmitted to the specimen (Fig. 7). Cantilever bending specimens are used for testing (Fig. 8).

5.2 Fluctuating tensile load fatiguing

Machine: High-frequency AMSLER pulsator Type 2HFP (Fig. 9), testing frequency 70 - 90 Hz, maximum load 20 000 N. The pulsator works on the resonance principle and is equipped with an electromagnetic system which provides the driving force. Specimen shape is shown in Fig. 10.

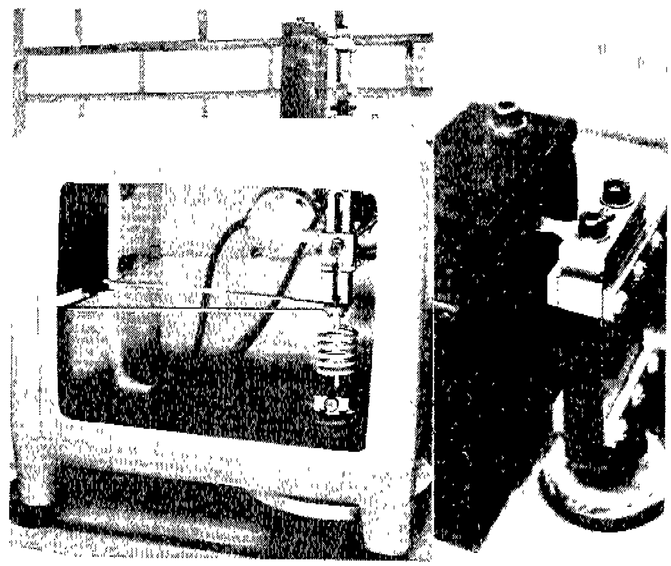

Fig. 7 Sonntag fatigue machine SF-2-U. Inside view with preload (left), testing fixture for cantilever bending specimen (right).

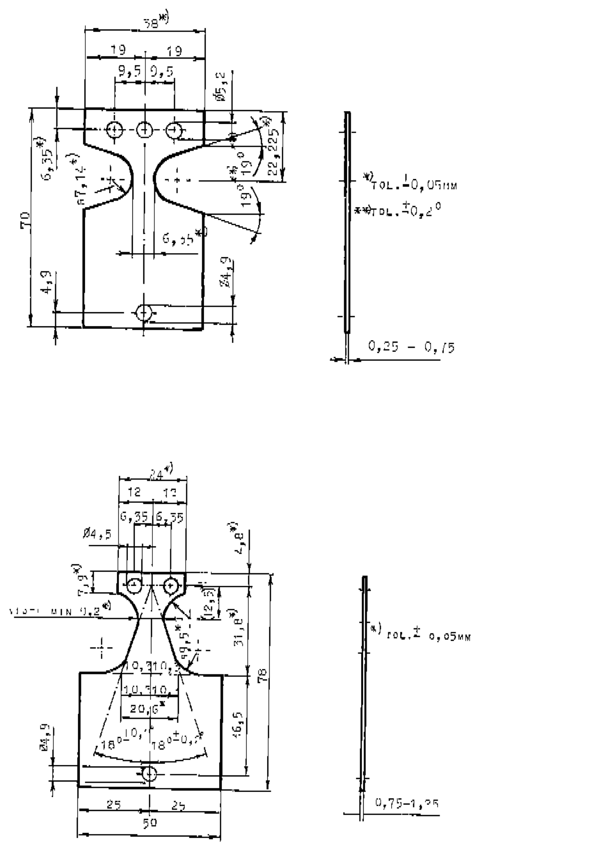

Fig. 8 Cantilever specimens for strip steel, thickness 0.25 - 0.75 mm (0.01 - 0.03 in) and 0.75 - 1.25 mm (0.03 - 0.049 in).

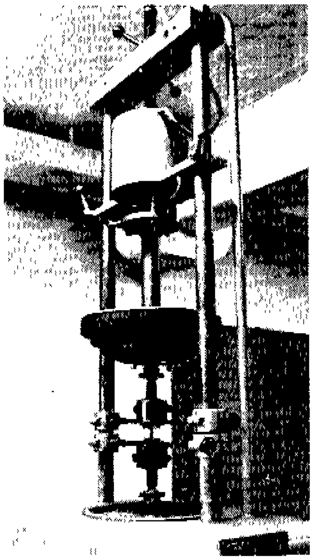

Fig. 9 AMSLER High-frequency pulsator Type 2HFP.

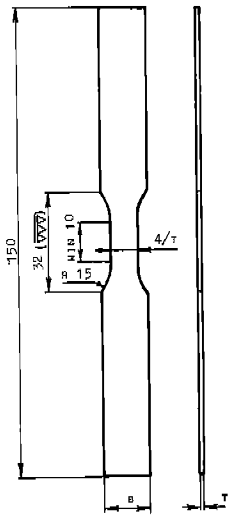

Fig. 10 Fatigue specimen for AMSLER.

5.3 Specimen preparation

The waist of all specimens is ground using a form-sharpened wheel. The edges are then ground with emery paper No. 220 - 400 - 600 in the longitudinal direction (6). The sharp edges are rounded off somewhat. Finally, the edges are polished with diamond paste. Every specimen edge is examined prior to testing in an ocular microscope at a magnification of 100 x. No transverse or longitudinal scratches should remain (Fig. 11).

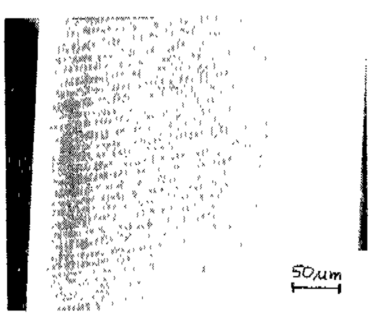

Fig. 11 Polished edge of fatigue specimen.

5.4 Fractography

The appearance of the fracture surface is studied in a scanning electron microscope. The purpose is to examine the cause of crack initiation. Knowledge gained in this manner is important in determining which of the external or internal defects control material fatigue. Fig. 12 and 13 show some fracture which were caused by surface defects or structural inhomogeneities.

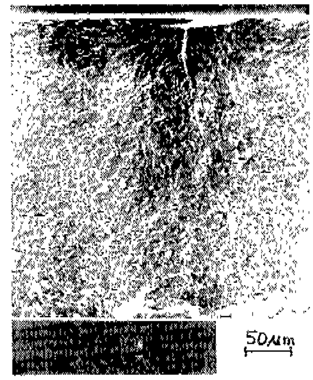

Fig. 12 Fatigue crack initiation at surface defect.

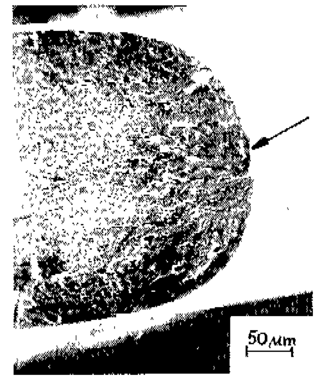

Fig. 13 Initiation of fatigue fracture at non metallic inclusion.

6 FATIGUE PROPERTIES OF UDDEHOLM VALVE STEELS

Testing was carried out at a room temperature of about 20°C (68°F) in a dry, non-corrosive atmosphere. The experimental material used to determine the fatigue limit at 2 x 10^6 loading cycles (see 3.1) comprised 30 - 40 specimens. The fatigue limit was defined as the stress at which 50 % of the specimens failed within 2 x 10^6 loading cycles. 50 - 80 specimens were tested to plot the S-N curve. The edges of all specimens except for the blanked ones were prepared as per 5.3. The surface was otherwise identical to the standard finish (7).

6.1 Bending fatigue testing

Reversed fatigue bending was carried out on UHB 20C and UHB Stainless 716 of thickness 0.30 mm (0.012 in) ultimate tensile strength 1 920 MN/m^2 (278 ksi) and 1 860 MN/m^2 (269 ksi), respectively (see the S-N curves, Fig. 14 and 15). UHB 15M and UHB 20C of thickness 1.25 mm (0.049 in) and 1.0 mm (0.039 in), respectively were also tested (see Fig. 16 and 17).

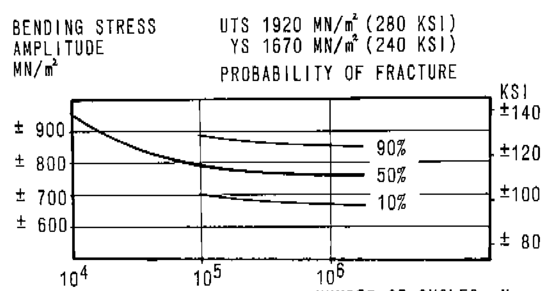

Fig. 14 S-N curves for UHB 20C, thickness 0.30 mm (0.012 in). Reversed bending, stress ratio R_s = -1.

The S-N curves are asymptotic, and a constant load corresponding to the fatigue limit of the material is attained at about 2 x 10^6 loading cycles. The staircase method provided a good estimate of the mean value. The estimation of high (e.g. 99 %) or low (1 %) confidence levels is, however, relatively poor, and other methods should be used for this purpose (3). Confidence levels for 10 and 90 % failure probability are specified in the diagrams.

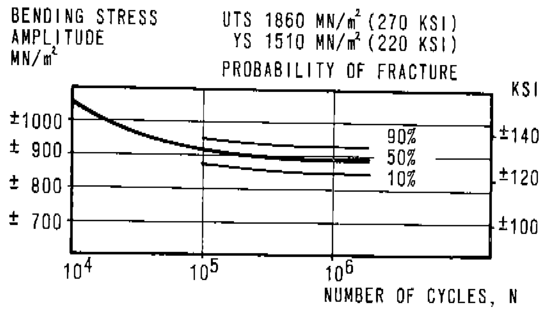

Fig. 15 S-N curves for UHB Stainless 716, thickness 0.30 mm (0.012 in). Reversed bending, stress ratio $R_s = -1$.

Compared to UHB 20C,UHB Stainless 716 exhibits a higher fatigue limit under reversed bending. This higher fatigue limit is due to dissimilarities in composition, structure and nature of the surface. Tests carried out on UHB 15M and UHB 20C with lower tensile strength, thickness 1.25 mm and 1.0 mm, respectively, gave a somewhat lower fatigue limit as compared to thickness 0.30 mm. The scatter of the measurement results was smaller.

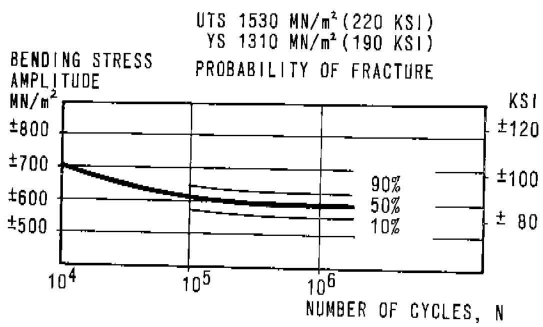

Fig. 16 S-N curves for UHB 15M, thickness 1.25 mm (0.049 in). Reversed bending, stress ratio $R_s = -1$.

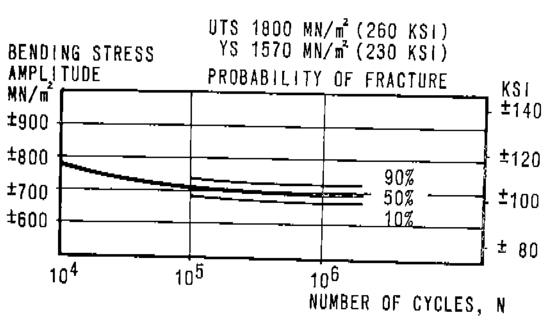

Fig. 17 S-N curves for UHB 20C, thickness 1.0 mm (0.039 in), Reversed bending, stress ratio $R_s = -1$.

6.2 Bending fatigue testing of tumbled specimens.

UHB 20C, thickness 0.30 mm, was fatigue-tested with a tumbled surface. Specimens were taken from the same strip material whose fatigue-testing is reported in Fig. 14. In addition, a series of specimens was subjected to excessive tumbling. The results are presented in the following table:

Table 2

UHB 20	Fatigue limit		Standard deviation	
	MN/m²	ksi	MN/m²	ksi
Standard surface	± 770	± 112	70	10
Tumbled	± 755	± 109	46	7
Excessive tumbled	± 750	± 109	201	29

Surface smoothness µm		µin		Residual stress (longitudinal direction)	
R_a	R_{max}	CLA	Max	MN/m²	ksi
0.06	0.8	2.4	31	-120	-17
0.16	2.4	6.3	94	-290	-42
0.18	2.1	7.1	83	-330	-48

Table 2 also reports the results of surface smoothness measurement perpendicular to the rolling direction and the residual stresses measured by X-ray for the different finishes. A deterioration of surface smoothness was noted between the standard polished finish (Fig. 18) and the tumbled finish. It appears probable that tumbling primarily improves edge quality by elimination notches due to blanking (8), while the surface properties have scarcely been improved with respect to fatigue, despite the inducement of higher compressive stresses. Furthermore, the relatively low compressive stresses in the valve material at hand are concentrated to a small surface layer of approx 5 - 10 µm. In view of the true defect size for the material and its application (1, 2, 8) it is doubtful that conditions at the tip of the defect which control crack initiation and thereby the strip material's fatigue properties are affected.

Syren, Wohlfahrt and Macherauch showed that besides surface condition the edge treatment has a strong influence on the bending fatigue. Material was carbon steel with 0.47 % C. On the other hand no remarkable effect of the residual stresses on the shape of the S-N (Wöhler) curve and the reversed bending fatigue strength has been found (9). In addition, residual stresses relax under dynamic loading (8, 10 - 12).

Surface studies of the tumbled specimens, conducted in the scanning electron microscope indicate the formation of surface defects as a result of excessive tumbling (Fig. 19). This latter phenomenon can also be related to the large standard deviation of the fatigue limit.

6.3 Tensile fatigue testing

In order to get a more complete picture of the fatigue properites of the valve steel, data obtained from tensile fatigue testing of UHB 20C and UHB Stainless 716, thickness 0.30 mm (0.012 in) is also presented (see Fig. 20 and 21). The results were virtually identical for both materials. During the uniaxial tensile loading which characterizes the testing of the strip material in the high-frequency pulsator, the influence of the surface on the fatigue properties of the material is less pronounced than during plane bending. Edge quality, however, is very important. Fig. 20 and 21 show the results which were obtained on blanked specimens, whose edges were riddled with cracks, burr and similar stress-raisers. This led to a sharp decrease of the fatigue limit to about half of that which was obtained on specimens whose edge was polished as per 5.3.

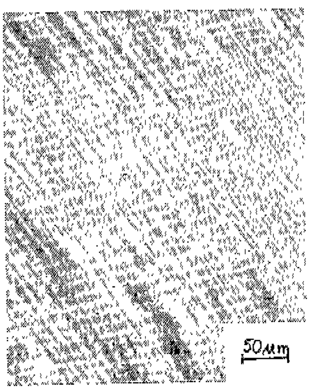

Fig. 18 Bright extra fine polished surface of UHB 20C.

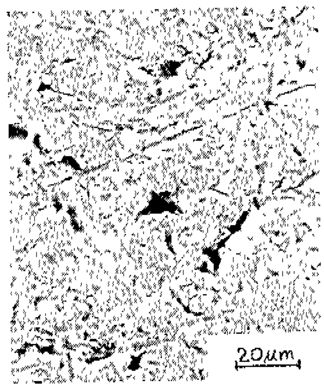

Fig. 19 Surface defects after excessive tumbling

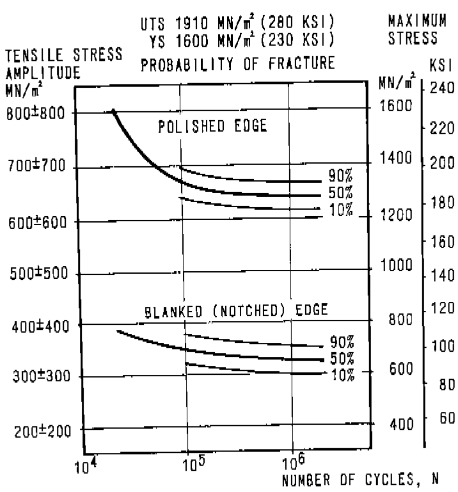

Fig. 20 S-N curves for UHB 20C, thickness 0.30 mm (0.012 in). Fluctuating tensile loading, stress ratio $R_s = 0$.

6.4 Crack growth at fatigue

If a crack is to be able to grow, the stress intensity factor at the tip of the crack must reach a threshold value. The crack growth rate da/dN in 1 % C and 0.35 % C, 13 % Cr steel as a function of the stress intensity factor range ΔK and its lower limit ΔK_T is shown in Fig. 22(13). ΔK_T for chromium steel was 3.8 $MN/m^{3/2}$ (3.5 $ksi\sqrt{in}$), while ΔK_T for carbon steel was determined at 4.5 $MN/m^{3/2}$ (4.2 $ksi\sqrt{in}$). After this, the crack grows in a stable manner, which can be described by the Paris equation (5), see 4.2.

$$da/dN = C\,(\Delta K)^n \qquad \text{equ. 1}$$

Testing was conducted with a fluctuating tensile load on SEN (Single Edge Notch) specimens.

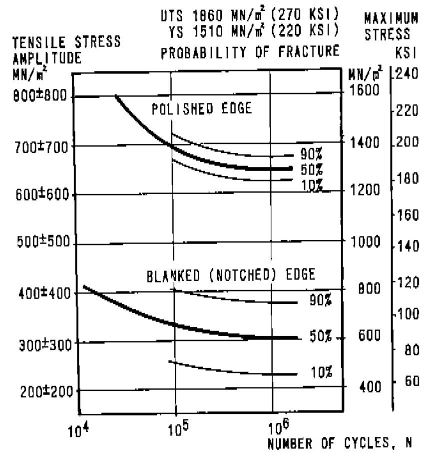

Fig. 21 S-N curves for UHB Stainless 716, thickness 0.30 mm (0.012 in). Fluctuating tensile loading, stress ratio $R_s = 0$.

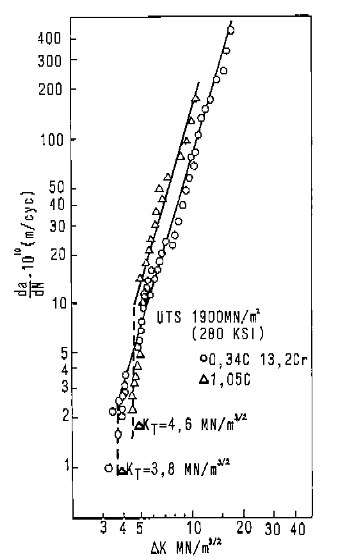

Fig. 22 Fatigue crack growth data for 1 % C and 0.35 % C, 13 % Cr steel.

7 FRACTURE MECHANICS PROPERTIES OF UDDEHOLM VALVE STEELS

In order to permit the quantification of the toughness properties of the thin strip for purposes of comparison, fracture mechanics testing was carried out. No attempt is made to establish valid K_{Ic} or K_c values. Instead, one value of the maximum stress intensity factor, which expresses the resistance of the material to unstable crack growth, is sought. Fracture mechanics testing was carried out under a plane-stress (slant fracture) or a "mixed mode condition", Fig. 23 (14). As is evident, the stress intensity factor is thickness-dependent.

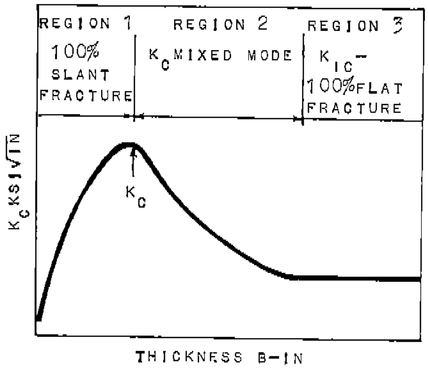

Fig. 23 Relationship between K_c and sheet thickness.

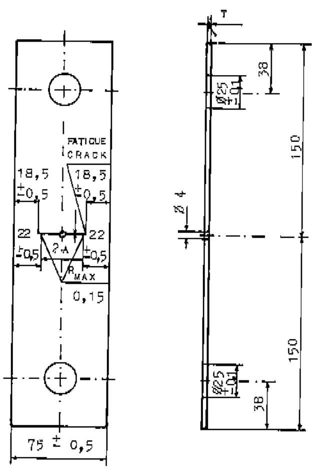

Fig. 24 Center-cracked tension specimen.

A CCT (Center Cracked Tensile) specimen was used for testing of UHB 20C and UHB Stainless 716 (Fig. 24). The set-up of the fracture mechanics test in the MTS machine is shown in Fig. 25. Stiffened springs on either side of the notch were used to prevent buckling of the specimen. A thin plastic film was applied between the springs and the specimen to reduce friction during loading to fracture.

The stress intensity factor K_I was calculated for the particular specimen geometry according to (15):

$$K_I = \frac{P\sqrt{a}\,Y}{BW} \qquad \text{equ. 2}$$

$$Y = 1.77 + 0.227\,(2\,a/W) - 0.510\,(2\,a/W)^2 + 2.7\,(2\,a/W)^3$$

P	Max. load
B	Strip thickness
W	Specimen width
2a	Crack length

K_{max} was iteratively corrected by inserting P_{max} in equ. 2 and correcting the crack length as per equ. 3, which applies to the plane-stress condition:

$$\bar{a}_i = a + \frac{1}{2\pi}\left(\frac{K_{i-1}}{\sigma_Y}\right)^2 \qquad \text{equ. 3}$$

$2a_i$	Corrected crack length
i	Iteration index
$2\bar{a}$	Measured crack length
σ_Y	Yield strength

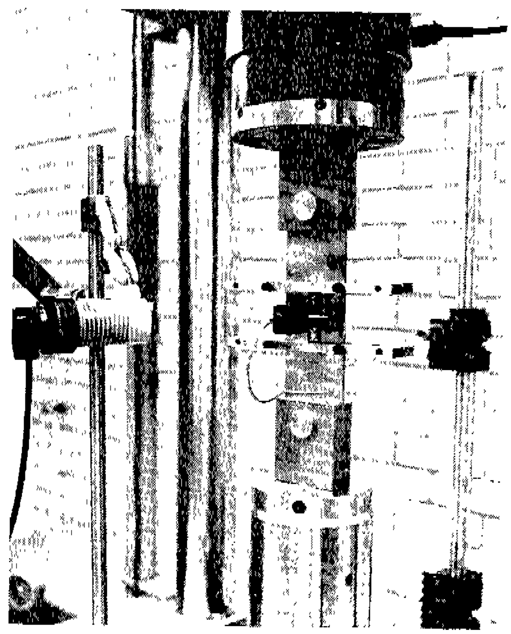

Fig. 25 Experimental set-up for fracture mechanical testing of strip steel.

The results as a function of the ultimate tensile strength are presented in Fig. 26. Both UHB 20C and UHB Stainless 716 of thickness 0.30 mm (0.012 (0.012 in) were tested. The fracture toughness of the material decrease rapidly with increasing tensile strength. It should, however, be pointed out that despite a tensile strength of around 2 000 MN/m^2, (290 ksi) the appearance of the fracture is characterized by plane-stress (Fig. 27). The small amount of flat fracture was noted for the tested thickness of UHB 20C only at a higher tensile strength.

UHB Stainless 716 displays a higher fracture toughness value K_{max} than UHB 20C. The results are not surprising in view of the differences in composition, structure and yield strength between the two materials.

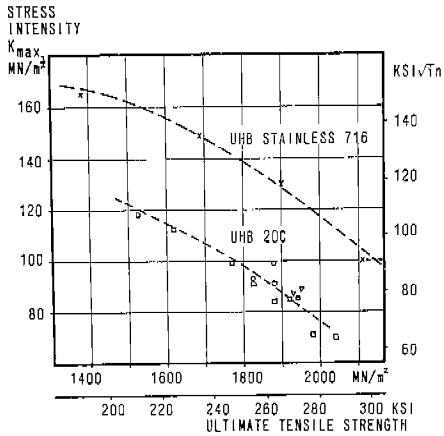

Fig. 26 Stress intensity factor versus ultimate tensile strength for UHB 20C and UHB Stainless 716. Thickness 0.30 mm (0.012 in).

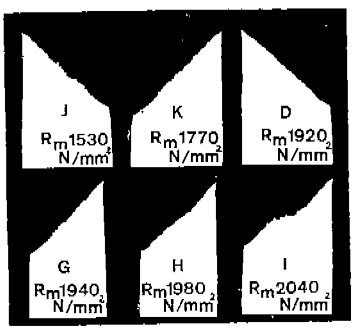

Fig. 27 Fracture surface observed in thin strip specimens illustrated in section views.

8 CONCLUSIONS

It should be pointed out that the fatigue and fracture mechanics data given here are not guarantee values for the material. The purpose of the presentation is to provide a rough idea of the properties of the strip material for the types of loads used in the laboratory.

It is difficult to transfer the laboratory results presented above directly to functioning valve reeds. The results obtained from, for example, reversed bending deviate from those which should be found for a functioning valve reed due to differences in loading geometry. In general, it can be said that the size of the stresses in the operating valve reed must be lower than the stresses corresponding to the fatigue limit. The stresses should be related to the desirable probability of the survival of the strip material with the same surface finish, dimension, tensile strength etc. Despite all limitations on the use of the data, knowledge of the fatigue properties of the strip material is considered to be useful as a guide in questions concerning such matters as choice of materials, yield strength, ultimate tensile strength, hardness, dimension, finish etc. Functional testing by means of, for example, an "accelerated life test" supplemented by a strain measurement in the surface of the valve can provide valuable information on how design geometry affects the stress pattern in the valve reed and can provide an opportunity to test the material under actual field conditions in a certain type of compressor (16 - 18).

It should be kept in mind that defects introduced during valve manufacture, assembly and operation, such as surface defects, blanking defects, corrosion etc. are, due to their stress-raising effects, of decisive importance in determining the service life of the reed (1, 2, 16, 17, 19). For a high-strength material such as flapper valve steel, the mechanisms at crack initiation are completely dominant in determining the fatigue performance of the material, (20), while subsequent stable and unstable crack growth are only of secondary significance.

7 REFERENCES

(1) D Goodchild and R Dusil:
Uddeholms Steel Research reports on causes of fracture in valve components made from cold rolled Steel strip. Sept 1973.

(2) R Dusil:
Case studies of Faults in Used Valves. Uddeholm Steel Research Report, FM73-016-10 (1975).

(3) A Guide for Fatigue Testing and Statistical Analysis of Fatigue Data, ASTM STP 91-A, 1963.

(4) H Bühler und W Schreiber:
Lösung einiger Aufgaben der Dauerschwingfestigkeit mit den Treppenstuffen Verfahren. Archiv für das Eisenhüttenwesen, 28 (1957) p. 153.

(5) P C Paris and F Erdogan:
A Critical Analysis of Crack Propagation in Cyclic Loaded Structures. Trans ASME serie D 85 (1963), p. 528.

(6) Handbook of Fatigue Testing. ASTM STP 566 (1974).

(7) Uddeholm cold rolled valve steels. Catalogue 1972.

(8) R Dusil:
Some Aspects of Blanking and Tumbling of Flapper Valves. Uddeholm Steel Research Report FM73-016-11 (1975).

(9) B Syren et al:
Influence of Residual Machining Stresses on the Bending Fatigue Strength of Steel Ck 45 in Annealed Condition. Arch. Eisenhüttenwes. 46 (1975) p. 735.

(10) J D Morrow et al:
Relaxation of Residual Stresses Due to Fatigue Loading. SAE Transaction 68 (1960) p. 41 - 48.

(11) S Taira and Y Murakami:
On the Changes in Residual Stresses Due to Repeated Stressing. The Third Japan Congress on Testing Materials. Met. Materials (1960) p. 52.

(12) A L Esquivel and K R Ewans:
X-ray Diffraction Study of Residual Macrostresses in Shot-peened and Fatigued 4130. Siemens Review, 37 (1970) p. 3 - 10.

(13) K-E Morén:
Stress intensity thresholds for two martensitic steels. Scand. J. Metallurgy 4 (1975) p. 255.

(14) A M Sullivan and C N Freed:
A Review of the Plane-Stress Fracture Mechanics Parameter K_c Determined Using and Center-Cracked Tension Specimen. Naval Research laboratory. Report 746. (1972).

(15) W F Brown and J F Scrawley:
Plane Strain Crack Toughness Testing of High Strength Metallic Materials. ASTM STP 410 (1967).

(16) R Cohen:
Valve Stress Analysis for Fatigue Problems. ASHRAE JOURNAL, June 1973, p. 57 - 61.

(17) R Gluck and R Cohen:
A Fatigue-Life Index as a Criterion for Evaluating Compressor Leaf Valve Design. ASME Paper No 66-WA/MD-10 (1966).

(18) P R Ukrainetz and R Cohen:
On Accelerated Life Tests for High Speed Compressor Valves. ASHRAE JOURNAL 8, No 1, (1966).

(19) W Soedel:
On Dynamic Stresses in Compressor Valve Reeds or Plates During Colinear Impact on Valve Seats. 1974 Purdue Compressor Technology Conference Proceedings, West Lafayette p. 319 - 328.

(20) A M Freudenthal:
New Aspects of Fatigue and Fracture Mechanics. Eng. Fracture Mech 6 (1974) p. 775.